Proceedings of the 2003 IEEE/RSJ International Conference on Intelligent Robots and Systems (IROS 2003), Las Vegas, NV, October 27-31, 2003.

Towards Grasping in Unstructured Environments: Optimization of Grasper Compliance and Configuration

Aaron M. Dollar and Robert D. Howe
Division of Engineering and Applied Sciences
Harvard University
Cambridge, MA 02138, USA
adollar@deas.harvard.edu, howe@deas.harvard.edu

Abstract - This paper examines the role of grasper compliance and kinematic configuration in unstructured environments, where object size and location may not be well known. A grasper consisting of two two-link planar fingers with compliant revolute joints was simulated as it passively deflects during contact with a target object. The kinematic configuration and joint stiffness values of the grasper were varied in order to maximize grasper workspace for a wide range of target object size. The results show a near-optimal result around the spring-rest angles of 25 and 45 degrees for the base and intermediate joints, respectively, when the joint stiffness ratio (base/intermediate) was small.

I. INTRODUCTION

One of the central challenges of robotics is grasping and manipulating objects in unstructured environments, where object properties are not known *a priori* and sensing is prone to error. The resulting uncertainty in the relationship between the object and gripper makes it difficult to control contact forces and establish a successful grasp or accurately position the object. One approach to dealing with this uncertainty is through compliance, so that positioning errors do not result in large forces and the grasper conforms to the object. This has most often been implemented through active control of manipulator impedance, and many studies have been devoted to impedance analysis and control techniques for robot arms and hands (e.g. Salisbury [1], Loncaric [2], Cutkosky and Kao [3], Lin et al [4], Bruyninckx et al. [5], Desai and Howe [6]). This approach is based on active use of position/velocity and force/torque sensor signals in the robot joints or end effector.

An alternative approach is the use of mechanical compliance in the manipulator structure. Ideally, carefully designed passive compliance can eliminate the need for a good deal of traditional sensor-based control. Recent results with legged robots demonstrate that judiciously tuned leg stiffness and kinematic configurations can permit stable high-speed locomotion over rough terrain using only open-loop commands (e.g. Clark et al. [7], Saranli et al. [8]). For manipulation, this approach is embodied in devices such as the Remote Center of Compliance that accommodate limited positioning errors (e.g. Nevins and Whitney [9], Schimmels and Huang [10]). These devices have achieved notable success in edge tracking and assembly tasks with small uncertainties.

In this paper, we explore the role of compliance and kinematic configuration in grasping in unstructured environments, where errors in sensing mean that object size and location uncertainty can span a wide range. In contrast to manipulators for unstructured environments that rely on active control for compliance (e.g. Francois et al. [11], Theobald et al. [12]), we are interested in passive joint compliance that results in large joint deflections and low contact forces, thus minimizing disturbance or damage to objects during the first phases of acquisition. In particular, we examine the performance of a two-fingered gripper as joint compliance and configuration are varied. Performance is compared on the basis of the maximum range of object size and location that can be successfully grasped. The results are analyzed to determine the ways that compliance and kinematic configuration contribute to grasping performance without the need for extensive sensing.

II. METHODS

The general problem of manipulation in unstructured environments is, by its very nature, so broad that assumptions are required to limit the scope of the problem to a tractable size. We thus select for this initial study a simple gripper with two fingers, each with two degrees of freedom (Figure 1). This gripper is perhaps the simplest configuration that is able to grasp a wide range of objects. This arrangement has been investigated in a number of contexts, including a design proposed by Hirose (Hirose and Umetani [13]), which uses only a single actuator to grasp objects. We assume that the links are rigid and that each joint of the gripper includes a passive linear spring in series with an actuator. Our goal is then to determine how variation in the joint stiffnesses and initial rest angles affect the ability to grasp objects. For this purpose, we must define the scenario in which the grasper will operate and determine its grasping ability by simulating the grasping process for a range of object sizes and locations.

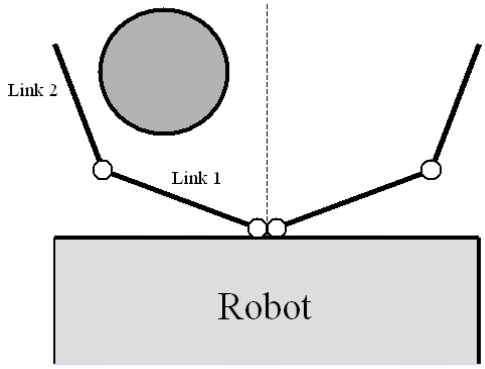

Figure 1: A grasper mounted on a robot vehicle approaching an object to be grasped. The grasper consists of two fingers, each a 2 degree of freedom planar manipulator.

A. Grasping Scenario

The basic grasping process follows a simple scenario. We assume that sensing (e.g. vision) provides rudimentary information about the target object location, and that the robot arm or vehicle moves straight towards this location. As the robot advances, the grasper comes into contact with an object with unknown properties and location. This results in contact forces, which deflect the grasper due to its compliance. The forward motion and joint deflection continues until one finger makes two-point contact with the object as described below. [See the attached video for example scenarios – (see video).]

At this point the joint actuators can be activated and both fingers brought into contact with the object.

To evaluate the potential of each grasper configuration to successfully grasp objects, we must define a "successful grasp." In an unstructured environment, the mechanical properties of the target object (particularly mass, frictional properties, and detailed shape) are uncertain, making it difficult to predict the precise finger configuration and grasp force necessary to secure the object. To circumvent this difficulty, we require an enveloping or form-closure grasp, in which the object is physically constrained by the grasper in all directions in the plane. For this simple grasper, form-closure equates to three- or four-point contact enclosing greater than 180 degrees along the object's surface. Therefore, at least one grasper finger must have two-point contact with the object. The possibility of achieving two-point contact on one grasper finger such that form-closure can be achieved is therefore the metric by which a successful grasp configuration is judged in this analysis. Figure 2 shows examples of successful and unsuccessful grasps.

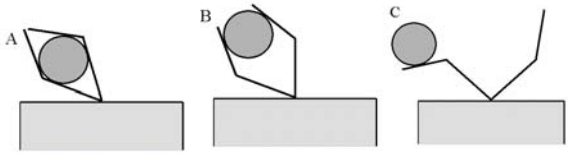

Figure 2: Example of a successful form-closure grasp (A), incomplete closure grasp (B), and unsuccessful grasp (C).

In order to simplify the analysis and simulation, we make a number of additional assumptions. First, we chose to ignore inertial effects and assume quasi-static conditions. To simplify the geometrical calculations, the links were assumed to be simple lines through the joint axes. The object to be grasped was assumed to be circular, simplifying the geometry, and unmovable, so that the contact forces with the gripper do not displace it. Also, the robot was assumed to move only in the forward direction, causing the distance of the object from the centerline to remain constant. Figure 3 depicts this scenario and relevant variables. Note that the base joint is the origin of the coordinate system.

B. Grasp analysis

Within this grasping scenario, we can examine the role of compliance and link configuration through simulation of the grasping process. We begin by analyzing the deflection of the grasper due to contact with the object as the robot advances.

In order to solve for the deflection behavior of the grasper for each case of object contact, we must solve for the inverse kinematics and balance the torque (due to deflection) in the compliant joints. Three cases of object contact on a finger are possible, each with different defining equations. The first case is object contact with the tip of the grasper. In the presence of friction, the tip will stick until static friction is overcome as the robot moves forward, begin to slide, and possibly transition to contact along the length of link 2 (the second case described below). Two-point contact will not often be achieved in this case. The second case is contact along the length of link 2 (pictured in figure 3). In this case the robot must continue moving forward, causing the object to slide along the length of link 2, until two-point contact is achieved, if at all. The third and simplest is contact on link 1. In this case, joint 2 can often be immediately actuated to achieve two-point contact and successfully grasp the object.

Except for the cases of tip contact, the contact with the object takes away a degree of freedom from the mechanism, giving a unique solution. However, to arrive at this solution, the inverse kinematics of the mechanism must be solved, along with a torque balance for each joint and equations describing the geometry of the grasper and object. The solution of these equations give the geometric

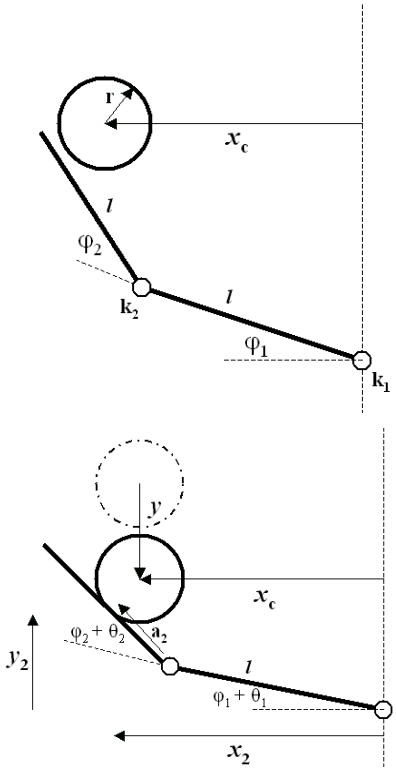

Figure 3: Diagrams describing the relevant terms used in the analysis of the manipulator before contact with the object (top) and after contact and deflection (bottom)

configuration of the grasper (i.e. the joint angles) for contact with an object of a certain radius at a given position as well as the contact point and the forces applied.

For the 2 DOF finger shown in figure 3, φ_1 and φ_2 are the spring rest link angles, θ_1 and θ_2 are the angular deflections from φ_1 and φ_2, y is the effective travel of the manipulator from the point of first contact, and k_1 and k_2 are the joint stiffness values. x_c is the distance from the center of the circle to the centerline of the grasper, r is the object radius, and y is the distance the manipulator has traveled since first contact with the object. l is the link lengths (which are set equal so that the origin can be reached), and a_2 is the variable contact length on the second link. The terms x_0,y_0, x_1,y_1 and x_2,y_2 are used to represent the coordinates of the initial contact point (x_0,y_0), and the contact points on each of the two links, respectively.

Contact at the tip of link 2

Two sets of equations are needed to describe this case. The first set describes tip contact with static friction, in which the frictional force is less than or equal to the coefficient of static friction times the normal force. Since the tip "sticks" to the object at the point of initial contact (described above), a closed-form solution to the joint angles can be found

$$\theta_2 = \gamma - \varphi_2 \qquad (1)$$
$$\theta_1 = \cos^{-1}\left(\frac{x_2}{2l\cos[0.5\gamma]}\right) - \frac{\gamma}{2} - \varphi_1$$
$$\gamma = \cos^{-1}\left(\frac{x_2^2 + y_2^2}{2l^2} - 1\right)$$

All of the terms in the above equations are known and are described above.

If the forces applied overcome static friction, dynamic or sliding frictional tip contact occurs. We can calculate the coordinates of the changing point of contact from the geometry of the grasper and the object when in contact with the object.

$$x_2 = r\sin\alpha + x_c$$
$$y_2 = y_0 - y + \sqrt{r^2 - (x_0 - x_c)^2} - r\cos\alpha \qquad (2)$$

where α is the angle between radius normal to the finger and the approach direction.

The changing contact point can also be calculated using the forward kinematics of the grasper:

$$x_2 = l\cos(\varphi_1 + \theta_1) + l\cos(\varphi_1 + \varphi_2 + \theta_1 + \theta_2) \qquad (3)$$
$$y_2 = l\sin(\varphi_1 + \theta_1) + l\sin(\varphi_1 + \varphi_2 + \theta_1 + \theta_2)$$

The component of the contact force tangential to the surface divided by the normal force is equal to the coefficient of kinetic friction

$$\frac{f_T}{f_N} = \mu_k \qquad (4)$$

And finally, the torque balance of the two joints yields

$$\frac{-k_2\theta_2}{f_N l} = \cos[\varphi_1 + \varphi_2 + \theta_1 + \theta_2 + \sin^{-1}\left(\frac{x_2 - x_c}{r}\right)] \qquad (5)$$
$$-\mu_k \cos[\frac{\pi}{2} - \varphi_1 - \varphi_2 - \theta_1 - \theta_2 - \sin^{-1}\left(\frac{x_2 - x_c}{r}\right)]$$

$$\frac{-k_1\theta_1}{f_N\sqrt{x_2^2 + y_2^2}} = \cos[\frac{\pi}{2} - \tan^{-1}\left(\frac{x_2}{y_2}\right) - \sin^{-1}\left(\frac{x_2 - x_c}{r}\right)]$$
$$-\mu_k \cos[\tan^{-1}\left(\frac{x_2}{y_2}\right) + \sin^{-1}\left(\frac{x_2 - x_c}{r}\right)]$$

Equations (1) - (5) can be solved simultaneously to find θ_1 and θ_2 as a function of object position in the approach direction (y).

In certain configurations, sliding tip contact can transition to contact along the length of link 2 as described below.

Contact along the length of link 2

If contact is initially along the length of link two, we can calculate the coordinates of the point of first contact from the geometry of the grasper and the object:

$$x_0 = r\sin(\varphi_1+\varphi_2)+x_c \qquad (6)$$
$$y_0 = l\sin\varphi_1+(x_0-l\cos\varphi_1)\tan(\varphi_1+\varphi_2)$$

Also from the geometry of the grasper and the object when in contact with the object, we can calculate the coordinates of the changing point of contact (shown in figure 3 above).

$$x_2 = r\sin(\varphi_1+\varphi_2+\theta_1+\theta_2)+x_c \qquad (7)$$
$$y_2 = y_0-y+r\cos(\varphi_1+\varphi_2)-r\cos(\varphi_1+\varphi_2+\theta_1+\theta_2)$$

The changing contact point can also be calculated using the forward kinematics of the grasper

$$x_2 = l\cos(\varphi_1+\theta_1)+a_2\cos(\varphi_1+\varphi_2+\theta_1+\theta_2) \quad (8)$$
$$y_2 = l\sin(\varphi_1+\theta_1)+a_2\sin(\varphi_1+\varphi_2+\theta_1+\theta_2)$$

where a_2 is the distance from joint 2 to the contact point. Finally, from the torque balance of the two joints, we get the following two expressions for the component of the force exerted normal to the object surface by the grasper. The second force relation is more complex because the force must be resolved to its component perpendicular to joint 1. The kinetic friction equation (4) holds in this case.

$$-k_2\theta_2 = \mathrm{f}_N a_2 \qquad (9)$$
$$\frac{-k_1\theta_1}{\sqrt{x_2^2+y_2^2}\,\mathrm{f}_N} = \sin[\varphi_1+\varphi_2+\theta_1+\theta_2+\tan^{-1}(\frac{x_2}{y_2})]$$
$$+\mu_k\cos[\pi-\varphi_1-\varphi_2-\theta_1-\theta_2-\tan^{-1}(\frac{x_2}{y_2})]$$

These equations allow us to relate the joint angles (θ_1, θ_2) and the applied force (F) to the robot travel (y), as a function of the design parameters (φ_1, φ_2, l, k_1/k_2) and the object properties (x_c, r). Note that a third set of equations describe contact on the first link (closest to the base). These are not presented here, but were derived similarly and are simpler.

C. Simulation

In the absence of a closed-form solution to the sets of equations, a numerical method was used to solve for the deflection behavior of the mechanism in the different contact states. The goal is to find the grasper configuration that maximizes the grasper workspace for various object sizes. To do this, the grasping scenario was simulated for a wide range of grasper parameter values and object location, measuring the grasper workspace.

The problem was simulated using Matlab (Mathworks, Natick, MA). The program solved the passive deflection behavior of the mechanism for incremented values of y (the robot travel) until two-point contact was established with the object, if occurring at all. A constraint was imposed on the travel of the fingers such that they do not deflect past the line horizontal from the base joint (i.e. $\varphi_1 + \theta_1 = 0$). Deflection past this line can be thought of as the fingers or object hitting the face of the robot structure.

If two-point contact occurs for a certain configuration, the program checks the locations of the contact points to verify that the grasp would enclose the object (i.e. the points of contact surround greater than 180 degrees of the object), allowing for a form-closure grasp to be attained. It was assumed that, due to symmetry, if the other finger were to be actuated at the point of two-point contact, the object would be in four-point form closure contact with the grasper [see video for example grasping scenarios from the simulation – (see video)]. It is also assumed that the fingers will not interfere with each other, as is the case if they are slightly offset in the out-of-plane direction.

The simulation was used to investigate the space of design parameters that can be chosen. The joint stiffnesses were applied to the model as a ratio, since the individual magnitudes only affect the magnitude of the applied force and not the deflection behavior of the mechanism. The static and kinetic friction coefficients were set equal to further reduce the dimension of the parameter space.

Due to the geometric constraints, only two of the three geometric parameters (φ_1, φ_2, l) can be chosen, as well as the ratio of k_1/k_2 and the coefficient of friction, μ. x_c and r are varied since the scenario is to grasp an unfamiliar object at an unknown location.

For this simulation, the lengths were normalized by l, the link length. Therefore, φ_1 and φ_2 were the geometric parameters varied. These angles were varied from 0 to 90 degrees at 5-degree increments. For both cases, the ratio k_1/k_2 was tested at values {0.1, 1, 10}. The coefficient of friction was tested at μ=2, based on previous studies that suggest high friction increases grasp stability (Shimoga et al. [14], Cutkosky et al. [15]).

The performance of each mechanism configuration was tested for a range of normalized object radius, r/l, (chosen to be {0.1, 0.5, 0.9}) and over the range of possible object location, x_c/l, (incremented from outside the grasping range toward the center by 0.01 until a successful configuration is reached). The maximum normalized distance of the object from the centerline for which a successful grasp was attained was recorded for each configuration. This value corresponds to the grasping range or the workspace of the grasper.

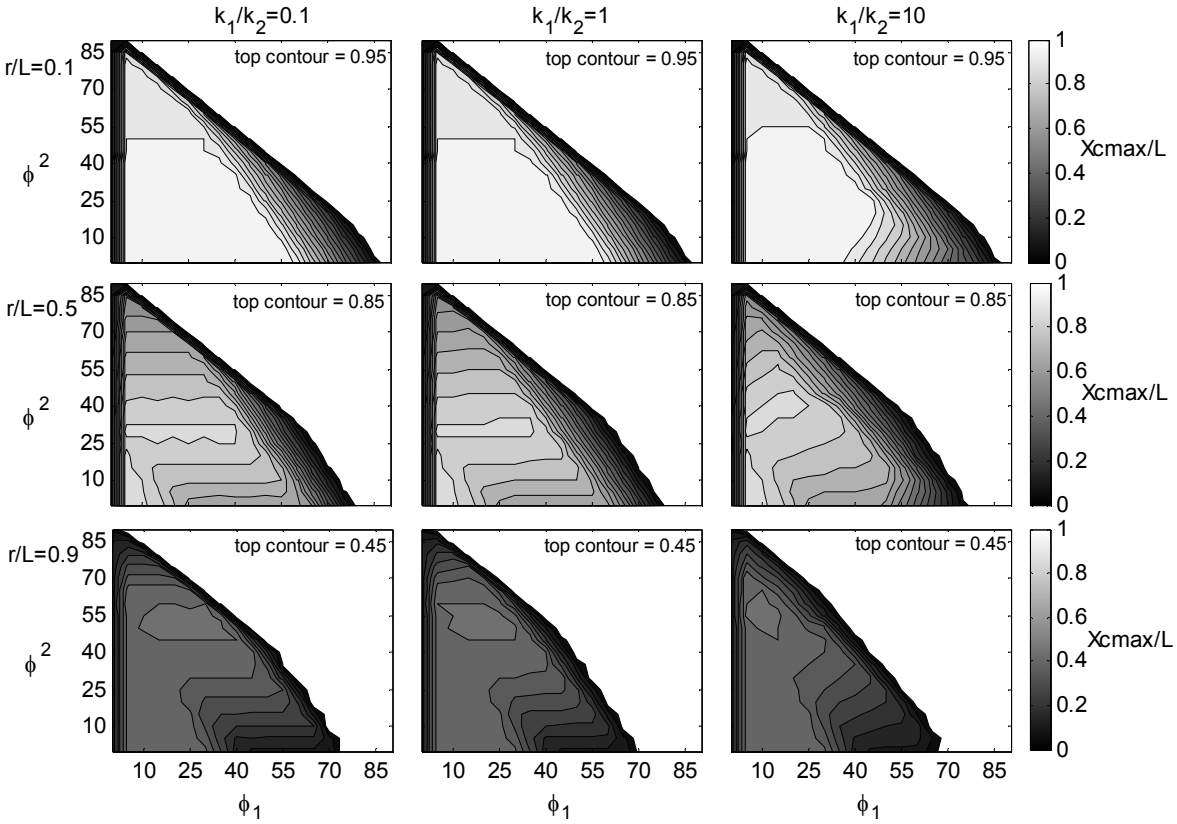

Figure 4: Simulation results for workspace $(x_c)_{max}$. Contours are in increments of 0.05.

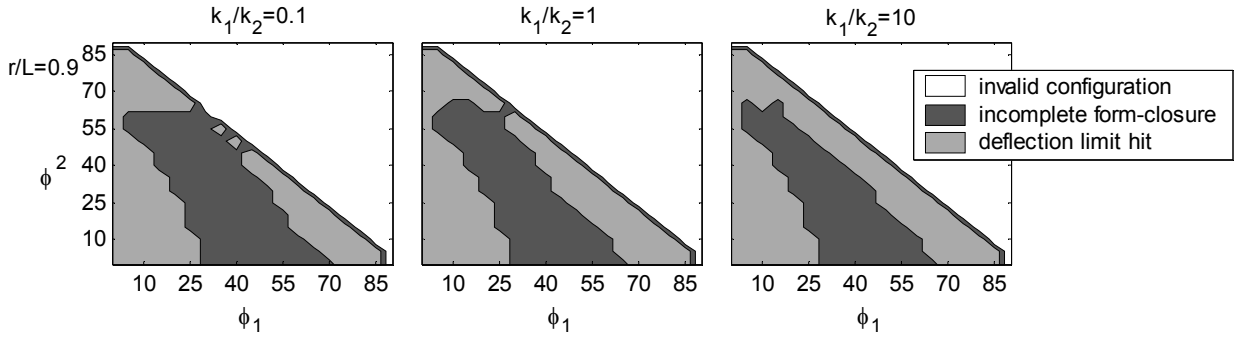

Figure 5: Description of modes of failure for the different regions of the configuration space for *r/l*=0.

III. RESULTS

Figure 4 shows the results of the simulation with the length terms normalized by the link length *l*. The nine plots represent combinations of three object radii and three stiffness ratios. For each plot, the axes are the rest angle for link 1 (φ_1) and link 2 (φ_2). The contours correspond to the values of $(x_c)_{max}$ (i..e. the grasper workspace) for each rest angle configuration, normalized by the link length.

Comparison of the plots across each row shows that increasing the stiffness ratio (k_1/k_2) does not affect the maximum value of the grasper workspace, $(x_c)_{max}$. Varying stiffness ratio does, however, affect the size of the optimum region for larger radius objects, as shown in the bottom two rows. In particular, a broader range of values for φ_1 produce the maximum workspace if the distal joint is stiffer than the base joint (i.e. $k_1<k_2$).

Comparing the columns of Figure 4, the optimum configuration space changes slightly with object radius, becoming smaller and moving toward increasing φ_2 for increasing object radius. Variation around these values is not large, however. For example, for *r/l*=0.9 the contour directly below the maximum value ($(x_c)_{max}$ */l*=0.40) is only 11% lower but contains a much larger region.

Figure 5 shows the failure modes for the configuration space at values of x_c just outside the successful grasp range for r/l=0.9. As an example, for φ_1=10 and φ_2=25, the grasp space is limited to around x_c/l=0.40 because outside of this range the grasper hits the deflection limit (i.e. the face of the robot structure). In another case, φ_1=25 and φ_2=40, the grasp space is limited to around x_c/l=0.40 because outside of this range the grasper cannot achieve form closure (i.e. two-point contact) on the object. The upper right half of each plot are invalid configurations for which $\varphi_1+\varphi_2$ exceed 90 degrees.

Note that the failure modes do not change significantly with stiffness ratio, except in the area of $25<\varphi_1<45$ and $25<\varphi_2<65$. In this region the initial contact with the object is tip contact with link 2. The mode switches from incomplete form closure to deflection limit because as k_1/k_2 increases, the increased stiffness of joint 1 prevents the tip from sliding, and sticks until hitting the deflection limit.

The failure mode for the best configurations is incomplete form closure. This lends weight to preferring these values since *force* closure might be achieved in practice, thus successfully grasping the object although outside the bounds of the assumed scenario.

IV. DISCUSSION

This study indicates that link configuration and stiffness ratios have a large impact on grasper performance, at least in terms of workspace. The optimum configuration allows the links to conform to even large objects, permitting a form closure grasp that is not possible for other configurations at large distances from the centerline. The workspace is particularly sensitive to variations in the distal joint rest angle, φ_2, while variations in φ_1 are not as significant for small values of the stiffness ratio k_1/k_2.

The stiffness ratio of the joints, k_1/k_2, does not affect the maximum grasper workspace that can be achieved. However, it does affect the size of the "sweet spot," and therefore should be minimized. Also, the magnitude of the individual joint stiffness values are directly related to the force applied to the object (i.e. lower absolute stiffness will result in lower applied forces). In order to avoid damaging or disturbing the target object, these values should be kept low. However, to avoid undesired resonant behavior, grasper dynamics should be taken into account when choosing these parameters.

A near-optimum link configuration across the parameter range studied, therefore, is around φ_1=25 and φ_2=45 for a stiffness ratio of k_1/k_2=0.1 (figure 6). This choice is within the optimum range for r/l=0.9 and is slightly off maximum for r/l=0.5. As noted above, φ_1 can vary across about 30 degrees with little effect on the workspace for this best stiffness ratio case.

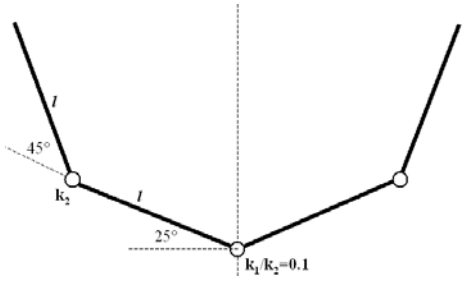

Figure 6: Optimum grasper configuration

The results presented above consider the behavior of the grasper for a wide range of object size with respect to grasper size. However, these results are most pertinent for the large object radius cases, as performance is largely unaffected by the configuration or stiffness parameters for the smallest objects (top row of Fig. 3). In addition, if the object size range is known, the gripper should be designed to approximate the size of the object. In this case, the results for the large object (i.e. r/l=0.9) are the most important.

This study was based on a specific grasping scenario, in order to limit the scope of the problem of grasping in an unstructured environment. A complete understanding of the issues will require exploration of alternative scenarios. For example, sensing and actuation are treated in a simplified fashion, with the assumption that once two-point contact is achieved, sensors will detect this condition, the robot will be stopped, and the other gripper finger actuated to form a force closure grasp. Important issues related to this include the type and amount of sensing needed. Is crude vision enough? Is contact sensing and proprioception such as joint encoders also needed? What is an appropriate actuation scheme incorporating the sensory information? The results presented here consider only the passive deflection of the mechanism (i.e. the "capture" phase) to maximize grasping space.

Another important assumption was the requirement of form closure for a successful grasp. We consider form closure to be the goal since the grasping environment is uncertain; however, in a real task, force-closure is sufficient for a stable grasp. The choice of a large value for the coefficient of friction can be debated as well, although informal studies suggest it does not have a large effect on grasp space.

Note that for the chosen geometric scheme of normalizing size parameters by the link length, l, the width of the grasper before contact varies for different combinations of φ_1 and φ_2. Normalization by an overall width parameter will enable comparison of grasper designs of similar width, which could be useful for designing a grasper to be used in a task with space constraints.

These results accord with recent results in legged locomotion research, where careful tuning of compliant robot legs has been shown to permit robust performance in unstructured environments with simple, open-loop control (e.g. Clark et al., 2001, Saranli et al., 2001). The analogy is particularly interesting in light of the fundamental differences between locomotion and manipulation. Unlike legs, which undergo fast, repetitive motion with relatively small variation in load and interaction with the environment, a compliant grasper will have highly variable interactions that must, to a considerable extent, utilize sensing. Further comparison of these modalities may lend insight into common passive "control" mechanisms.

IV. ACKNOWLEDGMENTS

This work was supported by the Office of Naval Research grant number N00014-98-1-0669.

V. REFERENCES

[1] K. J. Salisbury, " Active Stiffness Control of a Manipulator in Cartesian Coordinates," *19th IEEE Conference on Decision and Control*, Dec. 1980.

[2] J. Loncaric, "Geometrical Analysis of Compliant Mechanisms in Robotics," Ph.D. thesis, Harvard University, 1985.

[3] M. R. Cutkosky, I. Kao, "Computing and Controlling the Compliance of a Robotic Hand," *IEEE Transactions on Robotics and Automation*, vol. 5 (2), pp. 151-165, 1989.

[4] Q. Lin, J. Burdick, E. Rimon, "Computation and Analysis of Compliance in Grasping and Fixturing," *Proceedings of the 1997 IEEE International Conference on Robotics and Automation*, pp. 93-99, 1997.

[5] H. Bruyninckx, S. Demey, V. Kumar, "Generalized Stability of Compliant Grasps," *Proceedings of the 1998 International Conference on Robotics and Automation*, 1998.

[6] J. P. Desai and R. D. Howe, "Towards the development of a humanoid arm by minimizing interaction forces through minimum impedance control," *Proceedings of the IEEE International Conference on Robotics and Automation*, Seoul, Korea, May 23-25, 2001.

[7] J. E. Clark, J. G. Cham, S. A. Bailey, E. M. Froehlich, P. K. Nahata, R. J. Full, M. R. Cutkosky, "Biomimetic Design and Fabrication of a Hexapedal Running Robot," *Proceedings of the 2001 International Conference on Robotics and Automation*, Seoul, Korea, 2001.

[8] U. Saranli, M. Buehler, and D. E. Koditschek, "RHex: A Simple and Highly Mobile Hexapod Robot," *International Journal of Robotics Research*, vol. 20(7), pp. 616-631, July 2001.

[9] J. Nevins, D. Whitney, "Computer controlled assembly," *Scientific American*, vol. 238(2), pp. 62—74, 1978.

[10] J. M. Schimmels, S. Huang, "A Passive Mechanism that Improves Robotic Positioning through Compliance and Constraint," *Robotics and Computer-Integrated Manufacturing*, vol. 12 (1), pp. 65-71, 1996.

[11] C. Francois, K. Ikeuchi, M. Hebert, "A Three-Finger Gripper for Manipulation in Unstructured Environments," *Proceedings of the 1991 IEEE International Conference on Robotics and Automation*, pp. 2261-2266, 1991.

[12] D.A. Theobald, W.J. Hong, A. Madhani, B. Hoffman, G. Niemeyer, L. Cadapan, J.J.-E. Slotine, J.K. Salisbury, "Autonomous Rock Acquisition," *Proceedings of the AIAA Forum on Advanced Development in Space Robotics*, Madison, Wisconsin, August 1-2, 1996.

[13] S. Hirose and Y. Umetani, "Soft Gripper," *Proceedings of the 1983 ISIR*, pp. 112-127, 1983, cited in M. Kaneko, T. Tsuji, M Ishikawa, "The Robot that can Capture a Moving Object in a Blink," *Proceedings of the 2002 IEEE International Conference on Robotics and Automation*, pp. 3643-3648, 2002.

[14] K. B. Shimoga, A. A. Goldenberg, "Soft Materials for Robotic Fingers," *Proceedings of the 1992 IEEE International Conference on Robotics and Automation*, pp. 1300-1305, 1992.

[15] M. R. Cutkosky, J. M. Jourdain, P. K. Wright, "Skin Materials for Robotic Fingers," *Proceedings of the 1987 IEEE International Conference on Robotics and Automation*, pp. 1649-1654, 1987.